Free-induction-decay shape change by defect-induced quadrupole interaction*

M. K. Cueman, R. K. Hester,† A. Sher, and J. F. Soest
Department of Physics, College of William and Mary, Williamsburg, Virginia 23185

I. J. Lowe
Department of Physics, University of Pittsburgh, Pittsburgh, Pennsylvania 15260
(Received 18 June 1975)

The change in shape of the free induction decay (FID) in solids is calculated for the case of the point-defect-induced quadrupole interaction. The calculation agrees in form with the result of Fedders and predicts an FID of the form $V(t)\exp(-Kt^{3/2})$, where $V(t)$ is the FID with no quadrupole interaction (a perfect crystal), and K is proportional to the defect density. We adapt this theory to analyze FID data taken on the three isotopes in GaAs. The theory gives accurate fits to the data, and defect densities are calculated from the fit parameters for several thermally damaged samples and one doped sample. The principal purpose of this paper was the verification of the $t^{3/2}$ exponential dependence in the FID introduced by the quadrupole effect. The densities found for the damaged samples agree with the prediction of a thermodynamic calculation, for the smaller densities. Significant deviations occur at densities large enough that approximations made in the line-shape theory begin to break down. The magnitude of the deviations is larger than expected from the breakdown of theory alone, and may be evidence for the formation of singly charged vacancy pairs. The defect density measured for the doped sample is an order of magnitude less than the charge carrier concentration. This failure may be due to the breakdown in the theory or to donor clustering on dislocations.

I. INTRODUCTION

The effect on the NMR line shape of point defects in the crystal lattice of III-V compounds has been investigated in several recent articles.[1-4] Our own experimental research[1] in this area (this reference is hereafter referred to as HSSW) has used pulsed NMR to study GaAs in the technologically important low-defect-density regime of 10^{14}–10^{16} cm^{-3}.

Similar defect concentrations have been investigated by Sundfors[2] using cw NMR and nuclear-acoustic-resonance techniques. Defect densities several orders of magnitude greater, 10^{17}–10^{18} cm^{-3}, were measured by Potts and Pearson[3] using the Kossel line technique of x-ray diffraction.

In the past, the lack of an analytical form for the NMR line shape of a crystal with defects has limited the data analysis to comparison with moments of the line that can be calculated. This approach not only disregards much of the information contained in the NMR signal, but also forces one into the mathematically risky process of taking derivatives of an extrapolation of an empirical free-induction-decay equation. Further, one must then rely on theoretically calculated contributions to the second moments from all other line-broadening interactions in order to isolate the second moment owing to the quadrupole interaction.

Fedders[4] recently calculated a functional form for the quadrupole interaction contribution to the free induction decay (FID) of an NMR signal. This calculation permits a reexamination of the data in HSSW using the entire line shape in lieu of the moment analysis. This report constitutes a first test of this line-shape theory.

A brief description of the experiment is given in Sec. II. In Sec. III, a modification of Fedder's derivation is outlined for the change in the shape of the FID of zinc-blende structure single crystals owing to the presence of defects. The mechanism considered is the quadrupole interaction that is induced by the electric fields from charged point defects. Details of the calculation are presented in an Appendix.

Since one goal of this research is to develop a sensitive probe of crystal defect concentrations, the result derived in Sec. III is used to relate line shapes to defect densities in both thermally damaged and doped single crystals of GaAs. Most of the data used in this work were previously reported in HSSW. However, some of the data were retaken to improve the signal-to-noise ratio. The analysis is given in Sec. IV.

Finally, the theoretical and experimental limitations of this technique are discussed in Sec. V. The maximum measurable defect density is calculated for each of the three isotopes in GaAs. The functional forms of the change in the FID that would result from other damage-related interactions are discussed also.

II. EXPERIMENT

The experiment consisted of observing the FID following a 90° rf pulse, for each of the isotopes (^{69}Ga, ^{71}Ga, and ^{75}As, all with nuclear spin $\frac{3}{2}$), as

a function of crystal orientation in the Zeeman field. Data taken for several pure semi-insulating samples were reported previously in HSSW. Each of these samples was studied before and after thermal damage caused by quenching from a succession of temperatures in the range 500–700 °C.

Data from a silicon-doped crystal were gathered on the same apparatus reported in HSSW with two minor alterations. The sample probe and associated rf circuitry were changed from 50 to 93Ω characteristic impedance to allow a large filling factor in the sample coil despite a lossy sample. The tube preamplifier was replaced with an International Microwave Corp. Model No. S30ASA solid-state broad-band unit for improved stability. Each FID was recorded in the form of 1024 digitized and signal averaged points, typically 0.8 μsec apart.

III. THEORY

Since the difficulties inherent in calculating the entire NMR line shape are well known, this paper is limited to deriving only the change in the line shape resulting from the first-order quadrupole interaction. The theoretical result will then be used as the basis for comparison of signals from crystals that differ only in the amount of this interaction that is present.

It is assumed that the quadrupole interaction serves only to broaden the NMR frequency spectrum inhomogeneously. The effects of the quadrupole term on other elements of the total spin Hamiltonian, e.g., the dipole-dipole and indirect exchange interactions, are neglected. This approximation is equivalent to assuming that

$$[\mathcal{H}_Q, \mathcal{H}_{\text{tot}}] = 0 \ . \tag{1}$$

The effects owing to the breakdown of this approximation are discussed in Sec. V.

In this approximation, the NMR signal from a spin-$\frac{3}{2}$ nucleus will be the weighted sum of the contribution from the unperturbed ($\frac{1}{2}$ to $-\frac{1}{2}$) transition and the frequency shifted contributions from the ($\frac{3}{2}$ to $\frac{1}{2}$) and ($-\frac{1}{2}$ to $-\frac{3}{2}$) transitions. The latter may be written as a convolution of the spectral shape function $g(\omega)$ and the probability of a given frequency shift $p(\Delta\omega)$,

$$G(\omega) = 0.4g(\omega) + 0.6\int_{-\infty}^{\infty} p(\Delta\omega)g(\omega - \Delta\omega)d(\Delta\omega) \ . \tag{2}$$

In writing Eq. (2), it has been assumed that $g(\omega)$ is symmetric about the Larmor frequency.

The FID is the Fourier transform of the frequency spectrum. Equation (2) can be transformed to the time domain with the aid of the convolution theorem, giving

$$F(t) = 0.4f(t) + 0.6f(t)Q(t) \ , \tag{3}$$

where $F(t)$ is the observed FID, $f(t)$ is the Fourier transform of $g(\omega)$ (and thus the FID in the absence of quadrupole broadening), and

$$Q(t) = \int_{-\infty}^{\infty} d\omega \, e^{-i\omega t} p(\Delta\omega) \tag{4}$$

is the quadrupole modulation function.

A particular arrangement of defects will give a discrete frequency shift to one spin so that $p(\Delta\omega)$ can be represented by a δ function

$$p(\Delta\omega) = \delta\left(\omega - \sum_n \Delta\omega_n\right) \ , \tag{5}$$

where $\Delta\omega_n$ is the shift owing to defect n.

This δ function collapses the integral in Eq. (4) to the result

$$Q(t) = \exp\left[-i\left(\sum_n \Delta\omega_n\right)t\right] \ . \tag{6}$$

In an experiment one sees the sum of signals from nuclei that have many different arrangements of defects. Thus the observed signal is

$$\bar{F}(t) = 0.4f(t) + 0.6f(t)\bar{Q}(t) \ , \tag{7}$$

where $\bar{Q}(t)$ is a configuration average for the defect contributions to $\Delta\omega_n$ in Eq. (6). Details of the calculation of $\bar{Q}(t)$ are outlined in the Appendix.

The result of the configuration average is given by Eq. (A21), which allows one to express the quadrupole modulated FID as

$$F(t) = 0.4f(t) + 0.6f(t)e^{-Kt^{3/2}} \ , \tag{8}$$

where

$$K = \tfrac{4}{15}\rho_d(\pi e^* eQR/\hbar)^{3/2}\,(4\cos^2\theta - 3\cos^4\theta)^{3/4} \ . \tag{9}$$

In Eq. (9), ρ_d is the defect density, e^* is the effective charge of the defects, Q is the quadrupole moment of the observed nucleus, and R is the constant that relates the induced electric field gradients (efg) to an applied electric field.[5] The angle θ is the angle between the Zeeman field H_0 and the crystal $[1\bar{1}0]$ axis, for a rotation about a [110] axis that is held perpendicular to H_0.

IV. ANALYSIS

The theory in its simplest form permits comparison of the FID of a damaged crystal $D(t)$ to the FID of a perfect or virgin crystal $V(t)$,

$$D(t) = V(t)A'(0.4 + 0.6e^{-Kt^{3/2}}) \ , \tag{10}$$

where $K = K(\rho_d, \theta)$ and A' is a normalization factor.

In practice the FID of the undamaged crystal, $U(t)$, retained a significant quadrupole contribution owing to the native defect population, ρ_0. Thus, comparison of the laboratory signals $D(t)$ and $U(t)$ required solving two equations simultaneously to eliminate $V(t)$. Then

$$D(t) = U(t)\frac{A(0.4+0.6e^{-Kt^{3/2}})}{0.4+0.6e^{-K_0 t^{3/2}}}, \tag{11}$$

where K_0 is proprotional to the native defect density.

Using a three-parameter least-squares fit of Eq. (11), which could adjust A, K, and K_0, we matched the FID's from damaged crystals, $D(t)$, to FID's from undamaged samples at the same orientation. The fit values of K and K_0 yielded defect densities of the damaged and undamaged crystals simultaneously. The fits consistently gave defect densities of the undamaged crystals of $\rho_0 = 5.2\times10^{14}$ cm^{-3}.

This value of ρ_0 was adopted as a standard, and the analysis was repeated using a two parameter fitting routine which could adjust only the normalization A and the damaged crystal defect density via K. No appreciable increase in χ^2 was caused by freezing the third parameter.

The two illustrations in Fig. 1 are samples of this comparison process and are typical of the quality of fitting with Eq. (11). In Fig. 1(a) the distinctly different FIDs from damaged and undamaged crystals are plotted together without modification. The undamaged crystal signal in Fig. 1(b) is multiplied by the fit values of the modulation term in Eq. (11) to match it to the damaged crystal signal.

The angular dependence of the fit constant K shown in Eq. (A6) provides a second check of the validity of the theory. A least-squares fit of the values of K as a function of angle (illustrated in Fig. 2) was used to calculate an average value for the defect density of the damaged crystals. These values of defect density are listed in Table I. In calculating ρ_d from K we have used the electronic charge e for the effective charge e^*. Justification for this value is given in HSSW.

In the semi-insulating crystals, conduction-electron shielding of the point defects is not significant. Shielding owing to the dielectric constant of the medium is included in the measured value of R.[5] An extra factor of ϵ was included erroneously in the calculations in HSSW.

There is approximately 10% uncertainty in the measured defect densities owing to the standard deviation of the values of K as a function of angle. This probable error does not include error in the quantities that relate K to ρ_d, such as R and Q.

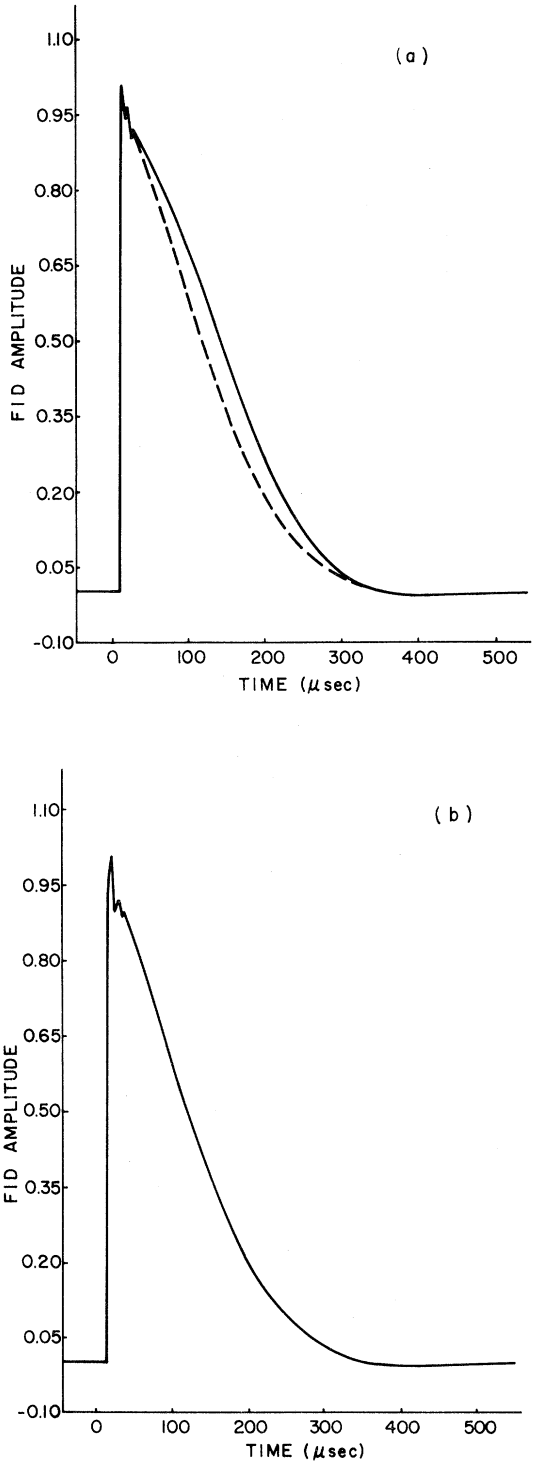

FIG. 1. (a) ^{71}Ga FID from an undamaged crystal with the Zeeman field parallel to the [110] direction (plain line) is compared with the ^{71}Ga FID from the same orientation of a sample quenched from 600 °C (broken line). (b) Similar to part (a) except the undamaged data has been modulated by the use of Eq. (11).

The product QR, measured by Gill and Bloembergen,[5] contributed a probable error of 30% to the absolute value of our measured ρ_d.

V. DISCUSSION

Using the chemical thermodynamics calculations of Logan and Hurle[6] as modified in HSSW, it is possible to determine the populations of As monovacancies created by thermal quenching. The result of this calculation is the line on Fig. 3. Since the theory presumes a perfect crystal before quenching, the native defect density is subtracted from the measured values for comparison to the theory. In Table I, the column labeled ρ_d (thermal) gives the results of this subtraction.

Experimental values for samples quenched from 600 °C and below, track the theoretical line fairly well, particularly considering there are no adjustable parameters except the FID normalization.

The experimental defect density from the sample quenched from 700 °C substantially undershoots the thermodynamic value. Furthermore, the defect density measured for the doped crystal is fully an order of magnitude less than the carrier concentration of $(3.9–5.1)\times10^{16}$ cm^{-3} measured by the manufacturer. These apparent failures must be examined in light of both experimental and theoretical limitations of this approach.

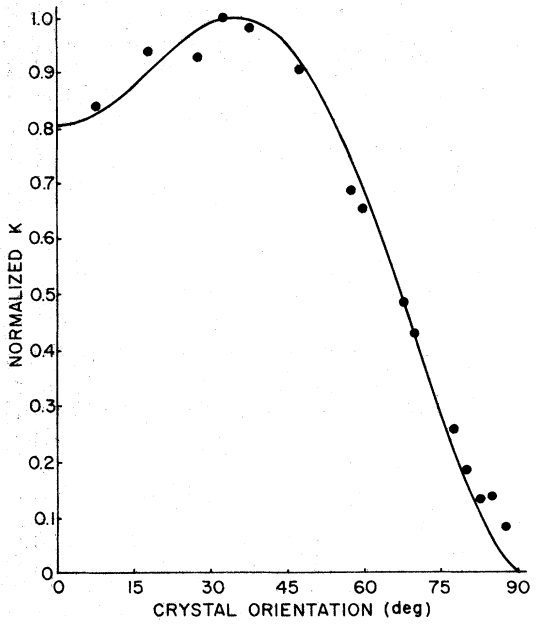

FIG. 2. Sample of the angular variation of the experimental fit parameter K compared to the theoretical orientation dependence from Eq. (11) (solid line). The data points were derived from ^{71}Ga FIDs of a crystal quenched from 600 °C.

Within the theory, higher defect densities imply faster decay of satellite contributions. This places more of the relevant part of the signal within the finite deadtime of the equipment. A reasonable estimate is that most of the quadrupole contribution has occurred by the critical time when the argument of the exponent in Eq. (8) equals −1. So, one can expect experimental saturation to set in when the critical time equals our experimental deadtime of about 20 μsec. If the full angular dependence of K is to be observed, this implies saturation densities of 34, 17, and 5.3×10^{15} cm^{-3} for ^{71}Ga, ^{69}Ga, and ^{75}As, respectively. Experimental saturation arguments could thus contribute to the anomalously low densities for M5D700 and EMC2 as measured by ^{69}Ga and ^{75}As. However, the ^{71}Ga densities appear to saturate at values lower than this estimate.

Concern that the quadrupole frequency shift may have placed an appreciable portion of the signal beyond the spectrometer's bandpass prompted construction of a fitting program that could adjust the weighting of the various transitions in the total signal (i.e., the factors 0.4 and 0.6). Bandpass

TABLE I. Defect densities of the experimental crystals as measured by the whole line shape technique.

Sample [a]	Quench temp °C	Isotope	ρ_d total [b] (10^{15} cm^{-3})	ρ_d thermal [c] (10^{15} cm^{-3})
M7	500	^{69}Ga	0.71	0.19
		^{71}Ga	•••	•••
		^{75}As	0.82	0.30
M2	550	^{69}Ga	1.0	0.48
		^{71}Ga	1.4	0.88
		^{75}As	0.88	0.36
M3	600	^{69}Ga	1.3	0.78
		^{71}Ga	1.8	1.3
		^{75}As	0.86	0.34
M7	600	^{69}Ga	1.7	1.0
		^{71}Ga	2.3	1.6
		^{75}As	1.3	0.58
M5	700	^{69}Ga	1.6	1.1
		^{71}Ga	1.7	1.2
		^{75}As	1.2	0.68
EMC2	Si doped	^{69}Ga	1.6	N/A
		^{71}Ga	2.0	N/A
		^{75}As	1.5	N/A

[a] For example, M7 designates crystal 7 from an ingot manufactured by Monsanto. These crystals were measured before and after damage was introduced by rapidly quenching them from the temperature listed in the second column. EMC refers to Electronics Material Corporation.

[b] ρ_d total is the defect density measured using Eq. (11).

[c] ρ_d thermal $=\rho_d$ total $-\rho_0$ where ρ_0 is the defect density prior to damaging. Note crystal M7 was damaged to 500 °C, then to 600 °C.

limitations would result in consistent deemphasis of the satellite transitions. No such pattern emerged in practice, and bandpass was judged not to be a problem.

Breakdown of the theory will occur when the initial approximation in Eq. (1) ceases to apply. The error terms will become appreciable when the quadrupole broadening approximates the broadening owing to other crystal Hamiltonian mechanisms. This condition is assumed to exist when the time required for the quadrupole modulation function $\overline{Q}(t)$ to decay to one-half is less than or equal to the time t^*, required for the pure-crystal FID $V(t)$ to reach its half height. Using Eq. (8), one can solve for the maximum value of K that satisfies this condition, which is

$$K_{\max} = \ln 6/(t^*)^{3/2} .$$

The experimental value of t^* is approximately 150 μsec, implying values of 3.8, 1.9, and 0.58×10^{15} cm^{-3} for ^{71}Ga, ^{69}Ga, and ^{75}As. These values are consistent with the saturation values of ρ_d shown in Fig. 3. At least in part the poor agreement for the high-damage investigations can be attributed to a breakdown of the theory itself.

Microscopically the theory breaks down when the field gradients owing to defects are large enough so that the changes in energy-level spacings from one nucleus to the nearest like nucleus are larger than the width of the levels. Then most of the mutual spin-flip terms of the dipolar broadening are no longer secular, and the linewidth of the separate transitions (i.e., $\frac{3}{2}$ to $\frac{1}{2}$, etc.) decreases by about 10%.[7] We have not generalized the theory to eliminate the troublesome approximation of Eq. (1), and cannot draw any conclusions with assurance, but it is hard to understand how such a small change in $V(t)$ can cause an apparent decrease in K by a factor of 10.

If one ascribes the deviation between the charged defect density and the Logan and Hurle calculation at 700 °C to the formation of singly charged As divacancies, then this deviation can be explained if the divacancy bonding energy is ≈ 1 eV. Both the theory and the data must be improved to confirm this speculation.

The Si-doped n-type sample EMC2 has both a higher mobility and a higher etch pit density than the original values for the Monsanto ingot. This would indicate that many of the donors are trapped along dislocations rather than being uniformly distributed throughout the bulk of the sample. This effect could explain the deviation between the measured defect concentration and the charge carrier concentration for this crystal.

The lower limit of defect densities that can be measured with confidence can be roughly placed by estimating that the modulation function $\overline{Q}(t)$ must have reduced the FID by at least 2% at t^* in order to be detected. This corresponds to defect densities on the order of 7×10^{13} cm^{-3}.

The principal purpose of this paper was the verification of the $t^{3/2}$ exponential dependence in the FID introduced by the quadrupole effect. This has been clearly established by the quality of the fits between the FID and the theory. In fact the theory continues to fit the shape of the curves well beyond the defect densities where its approximations break down.

As derived by Fedders,[4] the FID will be modulated, in general, by a term $\exp(-ct^{3/n})$ for field gradients that fall off as r^{-n}. We investigated the possibility of a r^{-3} dipole-field-induced efg effect by fitting an $\exp(-ct)$ dependence to our data. The resulting fits took three parameters to equal the two parameter performance of the $\exp(-Kt^{3/2})$ function, as measured by χ^2. An attempt to fit the data with an $\exp(-ct^2)$ function led to large χ^2.

APPENDIX

In order to calculate the configuration average, the frequency shift $\Delta\omega_n$ of one nucleus owing to

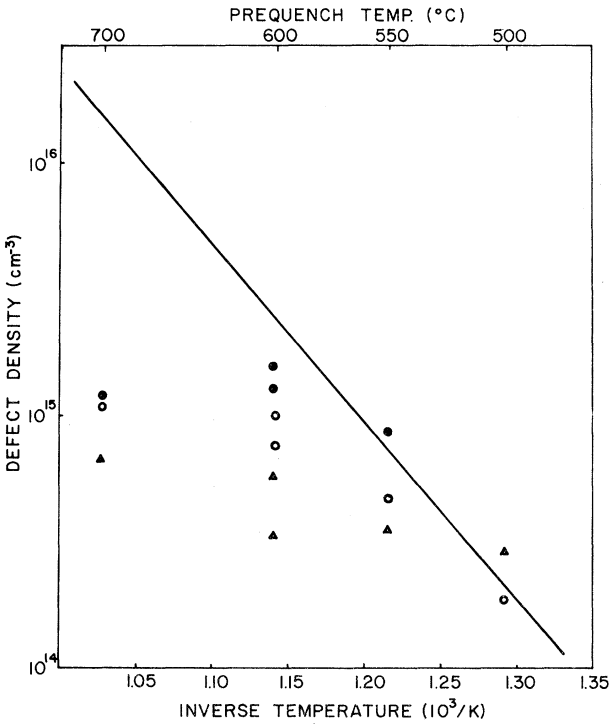

FIG. 3. Measured values of defect densities induced by thermal quenching are compared with the chemical thermodynamics calculation of HSSW (solid line). The open circles are measurements based on ^{69}Ga resonance data, solid circles on ^{71}Ga, and triangles on ^{75}As.

one defect must be found. For the first-order (high Zeeman field) quadrupolar interaction, the net shift of the satellite ($\frac{3}{2}$ to $\frac{1}{2}$) transition is[8]

$$\Delta\omega = \pm\, 2\omega_Q \tag{A1a}$$

where

$$\omega_Q = A\sum_{i,j} V_{ij}(3\gamma_i\gamma_j - \delta_{ij}) \tag{A1b}$$

and

$$A = eQ/[4I(2I-1)] \ . \tag{A1c}$$

The V_{ij} are the components of the efg tensor, the γ_i are the direction cosines of the Zeeman field with respect to the crystal lattice, and Q is the electric quadrupole moment of the spins I.

In the zinc-blende lattice, the efg tensor is induced by the electric fields from charge defects according to the relation[5]

$$V_{ij} = -R\sum_k \delta_{ijk}E_k \ , \tag{A2}$$

where E_k is the k component of an unshielded electric field from an effective point charge e^*, and $\delta_{ijk}=1$ if the indices i, j, and k are all different, and 0 otherwise. Substitution of Eq. (A2) into Eqs. (A1) yields

$$\Delta\omega = \pm\frac{2ARe^*}{r^2}\sum_{i,j,k}(3\gamma_i\gamma_j - \delta_{ij})\delta_{ijk}\Omega_k \ , \tag{A3}$$

where the Ω_k are the direction cosines of $\vec{E}$ at the nucleus. Eq. (A3) can be simplified and rewritten in the form

$$\Delta\omega = \alpha\cos\psi/r^2 \ , \tag{A4}$$

where

$$\alpha = 6ARe^*\Gamma \ , \tag{A5}$$

and ψ is an angle relating the efg tensor principal axes to the direction of the electric field. This angle will be averaged over in the configuration average so it need not be specified further. Γ is a function of the crystal orientation in the magnetic field

$$\Gamma = 2(\gamma_x^2\gamma_z^2 + \gamma_z^2\gamma_y^2 + \gamma_y^2\gamma_x^2)^{1/2} \ .$$

In the case of interest, the crystal is rotated about a [110] axis that is perpendicular to the Zeeman field. Then

$$\Gamma = (4\cos^2\theta - 3\cos^4\theta)^{1/2} \ , \tag{A6}$$

where θ is the angle between H_0 and the $[1\bar{1}0]$ direction.

To simplify the configuration average, the sample is assumed to be a sphere with the nucleus of interest in the center. The sphere has a radius $R \approx 0.5$ cm. Charge defects occur randomly throughout the sample, with the closest approach distance $r_0 \approx 2$ Å depending on which sublattice the defect resides.

If the defects are randomly located and statistically independent, except that no two are permitted to occupy the same site, the probability P_c of a given configuration of defects is given by a product of single defect probabilities,

$$P_c = \mathcal{P}(\vec{r}_1)d^3r_1\mathcal{P}(\vec{r}_2)d^3r_2\cdots = \prod_{n=1}^{N}\mathcal{P}(\vec{r}_n)d^3r_n \ ,$$

where $\mathcal{P}(\vec{r}_n)d^3r_n$ is the probability of a defect occuring in a volume element d^3r_n located at position $\vec{r}_n$, and N is the total number of defects. The probability density $\mathcal{P}(\vec{r}_n)$ is the same for each $\vec{r}_n$, namely,

$$\mathcal{P}(\vec{r}_n) = 1/V_0 \ ,$$

where

$$V_0 = \tfrac{4}{3}\pi R^3 - \tfrac{4}{3}\pi r_x^3 = \tfrac{4}{3}\pi R^3[1-(r_x/R)^3] \tag{A7}$$

is the free volume in which one defect may occur. Ordinarily the small excluded volume $\frac{4}{3}\pi r_x^3$ could be ignored, but in the limit $R, N \to \infty$ it contributes an important correction.

Now the configuration average becomes

$$\bar{Q}(t) = \int\int\cdots\int Q(t)\prod_{n=1}^{N}\mathcal{P}(\vec{r}_n)d^3r_n \ .$$

$$= \frac{1}{V_0^n}\int\int\cdots\int Q(t)\prod_{n=1}^{N} d^3r_n \ ,$$

where each integral is over the volume V_0. Substitution of $Q(t)$ from Eq. (6) gives

$$\bar{Q}(t) = \frac{1}{V_0^N}\int\int\cdots\int \exp\left(-i\sum_N \Delta\omega_n t\right)\prod_{n=1}^{N} d^3r_n$$

$$= \frac{1}{V_0^N}\prod_{n=1}^{N}\int \exp(-i\Delta\omega_n t)d^3r_n \ . \tag{A8}$$

Since the defects are randomly located, each of the N integrals in Eq. (A8) is identical and $\bar{Q}(t)$ simplifies to

$$\bar{Q}(t) = \frac{1}{V_0^N}\left(\int\exp(-i\Delta\omega t)d^3r\right)^N \equiv \left(\frac{1}{V_0}\mathcal{g}\right)^N \tag{A9}$$

Substitution for $\Delta\omega$ from Eq. (A4) and integrating over the angular portion gives

$$\mathcal{g} = 4\pi r_0\phi_0^{3/2}\int_{\phi_s^{1/2}}^{\phi_0^{1/2}}\frac{\sin y^2}{y^6}dy \ , \tag{A10}$$

where $\phi_0 \equiv \alpha t/r_0^2$ is the maximum phase shift from

resonance accumulated by a nucleus located at the closest possible distance from a defect. Similarly, $\phi_s \equiv \alpha t/R^2$ is the maximum phase shift for a nucleus at the center of the sample owing to a defect near the surface.

The quantity ϕ_0, found from the parameters in Eq. (A5), is a large number after a time on the order of 1 μsec. If one uses values of α and r_0 appropriate for GaAs, one finds

$$\phi_0 \approx 2\pi(40\text{MHz})t \approx 2.5\times10^8 t \ . \tag{A11}$$

In contrast, ϕ_s is a very small number throughout the FID, since

$$\phi_s/\phi_0 = r_0^2/R^2 \approx 10^{-14}$$

for a sample with $R = 2$ mm. Thus at the end of a FID lasting 1 msec,

$$\phi_s \approx 10^{-14}\phi_0 \approx 10^{-14}(2.5\times10^8)10^{-3} = 2.5\times10^{-9} \ .$$

Integrating Eq. (A10) by parts and using the approximations $\sin\phi_s \approx \phi_s$ and $\cos\phi_s \approx 1$ yields

$$g = \frac{4\pi r_0^3}{3}\left[\left(\frac{\phi_0}{\phi_s}\right)^{3/2} - \frac{3\sin\phi_0}{5\phi_0} - \frac{2\cos\phi_0}{5} - \frac{4}{5}\phi_0^{3/2}\phi_s^{1/2} + \frac{4\phi_0\sin\phi_0}{5} + \frac{8\phi_0^{3/2}}{5}\int_{\phi_s^{1/2}}^{\phi_0^{1/2}} \cos(y^2)dy\right] . \tag{A12}$$

The last term in Eq. (A12) can be replaced with a form of the Fresnel integral

$$\mathcal{F}(\phi_0) = \int_0^{\phi_0^{1/2}} \cos(y^2)dy \tag{A13}$$

introducing a small error.

Substitution for V_0 from Eq. (A7) and retaining terms of $O(1/R^3)$ or larger gives

$$g/V_0 = 1 + G(\phi_0)r_x^3/R^3$$

where

$$G(\phi_0) \equiv 1 - \frac{r_0^3}{r_x^3}\left(\frac{3\sin\phi_0}{5\phi_0} + \frac{2\cos\phi_0}{5} - \frac{4\phi_0^{3/2}\phi_s^{1/2}}{5} + \frac{8\phi_0^{3/2}\mathcal{F}(\phi_0)}{5}\right) . \tag{A14}$$

Finally, Eq. (A9) becomes

$$\bar{Q}(t) = [1 + G(\phi_0)r_x^3/R^3]^N \ , \tag{A15}$$

where N is the number of defects, typically on the order of 10^{15}. To complete the calculation, let $N \to \infty$ in such a manner that the defect density ρ_d remains constant:

$$\rho_d = N/V = 3N/4\pi R^3 = \text{const.}$$

In that limit,

$$\bar{Q}(t) = \lim_{\substack{R,N\to\infty \\ \rho_d = \text{const.}}} [1 + G(\phi_0)4\pi r_x^3/3N]^N = \exp[\rho_d v G(\phi_0)] \ , \tag{A16}$$

where

$$v = \tfrac{4}{3}\pi r_x^3 . \tag{A17}$$

For very short times the Fresnel integral in $G(\phi_0)$ approaches the square root of its argument, and other small angle approximations can be used to show

$$G(\phi_0 \to 0) \sim \text{const.} - t^2 \ .$$

Thus for short times, $\bar{Q}(t)$ approaches a Gaussian shape. However, the short time behavior is influenced most by nuclei with nearby defects, so the continuum average calculation is likely to be inaccurate for this time domain.

At long times, the Fresnel integral approaches a constant, and $G(\phi_0)$ becomes

$$G(\phi_0 \to \infty) \sim 1 - \frac{r_0^3}{r_x^3}\left(\frac{3\sin\phi_0}{5\phi_0} + \frac{2\cos\phi_0}{5} - \frac{4\phi_0\sin\phi_0}{5} + \frac{4\phi_0^{3/2}(\tfrac{1}{2}\pi)^{1/2}}{5}\right) . \tag{A18}$$

The last term finally dominates Eq. (A18), giving

$$\bar{Q}(t \to \infty) = e^{-Kt^{3/2}} \tag{A19}$$

where

$$K = \rho_d v \frac{r_0^3}{r_x^3}\frac{4(\tfrac{1}{2}\pi)^{1/2}}{5}\left(\frac{\alpha}{r_0^2}\right)^{3/2} . \tag{A20}$$

For the case of GaAs, it was shown in Eq. (A11) that ϕ_0 is large for times as short as 1 μsec, very early in the FID. Experimental limitations caused by a large piezoelectric response from the sample make it necessary to begin analyzing the data after $t = 20$ μsec, where $\phi_0 \approx 5\times10^3$. Thus the long time approximation is adequate for our data. This simplifies the analysis of the data, but at the price of loss of information about r_0.

Combining Eqs. (A20), (A19), and (A17), we conclude that the quadrupole modulation function can be written

$$\bar{Q}(t) = \exp[-\tfrac{4}{15}\rho_d(\pi e^* eQR/\hbar)^{3/2} \times (4\cos^2\theta - 3\cos^4\theta)^{3/4}t^{3/2}] . \tag{A21}$$

*Supported in part by NSF Grant No. DMR73-02365.

†Present address: Department of Chemistry and Research Laboratory of Electronics, MIT, Cambridge, Mass. 02139.

[1]R. K. Hester, A. Sher, J. F. Soest, and G. Weisz, Phys. Rev. B 10, 4262 (1974).

[2]R. K. Sundfors, Phys. Rev. 185, 458 (1969).

[3]H. R. Potts and G. L. Pearson, J. Appl. Phys. 37, 2098 (1966).

[4]Peter A. Fedders, Phys. Rev. B 11, 1020 (1975).

[5]D. Gill and N. Bloembergen, Phys. Rev. 129, 2398 (1963).

[6]R. M. Logan and D. T. J. Hurle, J. Phys. Chem. Solids 32, 1739 (1971).

[7]A. Abragam, *The Principles of Nuclear Magnetism* (Oxford U.P., London, 1964), p. 130.

[8]M. H. Cohen and F. Reif, Solid State Phys. 5, 322 (1957).